

# No nearby counterparts to the moving objects in the Hubble Deep Field

Chris Flynn<sup>1</sup>, J. Sommer-Larsen<sup>2</sup>, B. Fuchs<sup>3</sup>, David S. Graff<sup>4</sup> & Samir Salim<sup>4</sup>

<sup>1</sup>*Tuorla Observatory, Piikkiö, FIN-21500, Finland*

<sup>2</sup>*Theoretical Astrophysics Center, Juliane Maries Vej 30, Copenhagen, Denmark*

<sup>3</sup>*Astronomisches Rechen-Institut, Mönchhofstrasse 12-14, Heidelberg, Germany*

<sup>4</sup>*The Ohio State University Depts. of Physics and Astronomy, Columbus, OH 43210, USA*

28 March 2018

## ABSTRACT

Ibata et al (1999) have recently discovered faint, moving objects in the Hubble Deep Field. The quantity, magnitudes and proper motions of these objects are consistent with old white dwarfs making up the Galactic dark halo. We review a number of ground-based proper motion surveys in which nearby dark halo white dwarfs might be present, if they have the colours and absolute magnitudes proposed. No such objects have been found, whereas we argue here that several times more would be expected than in the Hubble Deep Field. We conclude it is unlikely that hydrogen atmosphere white dwarfs make up a significant fraction of the halo dark matter. No limits can be placed yet on helium atmosphere dwarfs from optical searches.

**Key words:** Galaxy – dark matter; Galaxy – structure

## 1 INTRODUCTION

Ibata et al (1999, hereafter IRGS99) have detected faint moving objects in the Hubble Deep Field (HDF). These objects have proper motions, apparent magnitudes and colours which are consistent with a Galactic dark halo made of old white dwarfs (WDs).

There are however reasons to suppose that white dwarfs make up only a limited amount of dark matter. They would over-pollute the Universe with carbon by a factor of 100 (Fields, Freese & Graff 1998). Although Chabrier (1999) has suggested that the above result may be model dependant, robust limits on the cosmic density of white dwarfs can be placed using helium and deuterium abundances (Fields, Freese & Graff 1999) and limits on background infrared photon number density (Graff, Freese, Walker & Pinsonneault 1999). These limits caused Hansen (1999a) to postulate the existence of beige dwarfs, degenerate massive objects that are not stellar remnants, and would escape the above restrictions. None of these objections are so robust that ways of circumventing them cannot be found. Some of the standard objections to white dwarfs as the halo dark matter are discussed by Richer (1999).

If the IRGS99 objects are halo white dwarfs, several nearby counterparts to such objects might be located in ground-based, wide area, proper motion surveys, in which they would appear as faint, high proper motion objects. Several such white dwarfs may have been found already. Hodgkin et al (1999) have followed up the Hambly et al

(1999) discovery of a very cool, halo white dwarf candidate. The object is at a distance of  $28 \pm 4$  pc and has velocity components consistent with belonging to a halo population. Harris et al (1999) have also located a very, low luminosity cool, white dwarf, although it's population type (disk or halo) is not yet known.

Such objects could be related to the objects found by IRGS99. In this paper, we examine the IRGS99 proposed population of dark halo white dwarfs by searching for nearby counterparts in existing, ground-based proper motion surveys. We find no candidate counterparts, although the volume probed by these surveys appears to be significantly larger than that probed by the Hubble Deep Field.

The power of a survey to detect objects of absolute magnitude  $M$  visible to limiting magnitude  $m$ , assumed to have a constant density is the effective volume of the survey,

$$v_{\text{eff}} = \frac{\Omega}{3} 10^{0.6(m-M)+3} \epsilon \text{ pc}^3. \quad (1)$$

where  $\epsilon$  is the efficiency (completeness) of the survey and  $\Omega$  its solid angle in steradians.

We examine two photographic surveys of proper motions, the Luyten Half Second Catalogue (1979, LHS) and the Knox, Hawkins & Hambly (1999, KHH). We show that both surveys have greater power to detect intrinsically faint high proper motion objects than the IRGS99 survey.

In neither ground-based survey do we find candidates for local counterparts to the proposed dark halo WDs in HDF. The probability of finding objects in the less powerful

HDF and not in the ground-based surveys is low, suggesting that the HDF objects are not dark halo white dwarfs.

This paper is organised as follows. In section 2 we discuss how to locate nearby counterparts to the proposed white dwarfs in proper motion surveys. In section 3 we search two such surveys, but find no candidates for such objects, while also demonstrating that both surveys would be more efficient at locating them than HDF itself. In section 4 we discuss our results in terms of models of cooling white dwarfs, and in section 5 we draw our conclusions.

## 2 PROPER MOTION SEARCH FOR DARK HALO WHITE DWARFS

Several authors have already searched for possible nearby dark halo objects, but have found no candidates, allowing an upper limit to be placed on their luminosity. The Luyten Half Second Catalog (LHS) has been analysed in this manner by Graff, Laughlin and Freese (1997), Fuchs and Jahreiß (1998) and Hansen (1999b). We follow here a similar approach as these authors while adapting it to the particular details of the IRGS99 proposal.

Assuming that some fraction  $F_{WD}$  of the dark halo is composed entirely of white dwarfs of mean mass  $M_{WD}$ , and that  $F_H$  of these dwarfs have hydrogen atmospheres, then the number  $N_{WD}$  of WDs we expect in the survey is:

$$N_{WD} = \frac{\rho_H}{M_{WD}} v_{\text{eff}} F_{WD} F_H. \quad (2)$$

where  $\rho_H$  is the local halo dark matter density. The dark halo is here assumed to have constant density, an adequate approximation out even to the range of the HDF, a kiloparsec from the Sun.

In two of the proper motion surveys discussed in the next section, there is an upper limit on the detectable proper motion  $\mu_{\text{max}}$ . In order to estimate the number of WDs with proper motions  $\mu < \mu_{\text{max}}$ , we assume the dark halo WD system is an isothermal sphere and that the 1-D velocity dispersion is  $220/\sqrt{2} = 156 \text{ km s}^{-1}$ . We assume the system is non-rotating, has local density  $\rho_H = 0.0076 \text{ M}_{\odot} \text{ pc}^{-3}$ , and that the mean WD mass is  $M_{WD} = 0.66 \text{ M}_{\odot}$ . We then determine the fraction of stars with proper motion  $\mu < \mu_{\text{max}}$  from the velocity distribution, while accounting for the Solar motion (i.e. we use Eq. 6 of Fuchs and Jahreiß 1998).

We search for nearby counterparts to the proposed HDF white dwarfs using the reduced proper motion,  $H$  (Luyten 1922, Evans 1992), which is the proper motion equivalent of absolute magnitude. For a star of absolute magnitude  $M$  and transverse velocity  $V_T$  (in  $\text{km s}^{-1}$ ), or apparent magnitude  $m$  and proper motion  $\mu$  (in  $\text{arcsec/year}$ ),  $H$  is

$$H = M + 5\log V_T - 3.379 = m + 5\log \mu + 5. \quad (3)$$

The reduced proper motions of the objects detected by IRGS99 in the HDF lie in the range  $24 < H_R < 26.5$ , as expected for objects with velocities characteristic of the dark halo and absolute magnitude at  $M_V \approx 17.5$ , (typical of the WDs proposed by IRGS99). Nearby counterparts to the HDF objects would also have reduced proper motions in this range.

## 3 THE THREE PROPER MOTION SURVEYS

We describe three surveys in which one can search for dark halo white dwarfs, two of which are ground-based and would locate nearby objects, and the third being the HDF itself (which has been searched by IRGS99). For each survey we calculate the effective volume probed. For the two ground-based surveys we search for but locate no dark halo white dwarf candidates.

### 3.1 The Hubble Deep Field

The Hubble Deep Field is the deepest search for any object, and covers a comparatively small solid angle, only  $4.4 \text{ arcmin}^2$ , or  $5 \times 10^{-8}$  of the angle covered by the larger of the two ground-based surveys (LHS). IRGS99 effectively run two experiments in searching for faint moving objects in HDF. They are most confident of their results for  $I < 28$ , and find two objects with  $I < 28$ . One of the objects varies in magnitude, and has the wrong  $B - V$  colours to be a white dwarf, leaving one good candidate object, 4-551. Extension of the survey out to  $I < 29$  reveals three additional candidates, though only one of these has a secure proper motion. The completeness of the Ibata et al survey is  $42 \pm 2\%$  for objects in the range  $27 < I < 28$ . The effective volume probed by HDF (using eqn 1) for objects at  $M_V = 17.5$  is  $v_{\text{eff}}^{\text{HDF}} = 225 \times 0.42 = 95 \text{ pc}^3$ . Conservatively, no correction has been included for the proper motion window of the HDF survey even though the measured proper motions are only  $\sim 2$  times larger than the minimum proper motion. IRGS99 do not discuss the upper proper motion limit of their survey, but it is likely to be much larger than the proper motions of the WDs.

### 3.2 ESO/SERC Area 287

Knox, Hawkins and Hambly (1999, hereafter KHH) have recently surveyed “ESO/SERC Area 287”, searching for faint high proper motion objects in order to locate the end of the disk white dwarf cooling sequence. They used about 100 UK Schmidt  $R$ -band exposures taken at a range of different epochs, which they stacked in three different manners either to go as deep as possible ( $R = 22$ ) or to be able to recover stars with high proper motions ( $10 \text{ arcsec/yr}$ ).

The three KHH proper motion experiments have different apparent magnitude  $R$ -band limits and upper proper motion limit  $\mu_{\text{max}}$ , and are denoted by (i), (ii) and (iii). Hambly (1999, private communication), has undertaken a careful re-analysis of the original data as a result of the IRGS99 results, and has advised us that the effective area of the survey should be conservatively set at 12 square degrees. The three experiments are summarised in Table 1, where we show the upper limit on proper motion  $\mu_{\text{max}}$ , the  $R$ -band apparent magnitude limit and effective volumes probed for each survey (including the effect of the proper motion window)  $v_{\text{eff}}$ . The most effective of the surveys is (i), for which  $v_{\text{eff}}^{\text{KHH}} = 198 \text{ pc}^3$  for white dwarfs at  $M_R = 17.5$ .

KHH show reduced proper motion in the  $R$ -band,  $H_R$  versus colour diagrams for their sources (their figures 9, 10 and 11). Inspection of their plots shows there are no sources with  $H_R > 24$ , (blue or otherwise). Almost all their sources have  $H_R < 20$  (as expected for late type dwarfs and disk

**Table 1.** Three proper motion surveys of ESO/SERC field 287 from Knox et al (1999), showing the upper proper motion limit  $\mu_{\max}$ , apparent  $R$ -band magnitude limit, fraction of sources expected in the proper motion window  $\epsilon$  (i.e. with  $\mu < \mu_{\max}$ ) and the effective volume  $v_{\text{eff}}$  for WDs at  $M_R = 17.5$

ID	$\mu_{\max}$ arcsec/yr	$R_{\text{lim}}$	$\epsilon$	$v_{\text{eff}}$ $\text{pc}^3$
(i)	10	21.2	1.00	198
(ii)	1.9	21.2	0.83	168
(iii)	0.5	22.0	0.24	146

white dwarfs). We conclude there are no candidate dark halo WDs in KHH.

### 3.3 Luyten Half Second Survey

The Luyten Half Second catalog (LHS — Luyten 1973) is a proper motion survey of most of the sky, complete in the range  $0.5 < \mu < 2.5$ , which was obtained by blinking Palomar plate pairs. Dawson (1986) has studied in detail the completeness of the LHS, finding that it is 90 % complete to Luyten  $R$ -band magnitude  $R_L = 18$  (for declination  $\delta > -30^\circ$ , and Galactic latitude  $|b| > 10^\circ$ ).

Salim and Gould (1999) have recently studied the completeness of the NLTT (“New Luyten Catalog of stars with proper motions larger than Two Tenths of an arcsecond”) in order to estimate the self lensing rate of field stars for astrometric microlensing. The NLTT is the extension to lower proper motions of the LHS catalog, and we have used the NLTT to determine the completeness of LHS. We find that LHS is 60% complete down to Luyten  $R$ -band magnitude  $R_L = 18.5$ . In Appendix A, we give a detailed presentation of this determination. Furthermore, in Appendix B, we calibrate the Luyten  $R$ -band magnitude,  $R_L$ , finding that it is actually closer to Johnson  $V_J$  than to Cousins  $R_C$ . The calibration is

$$R_L = V_J - 0.37(V_J - R_C) + 0.06. \quad (4)$$

This relation allows us to compare the LHS survey directly with HDF’s  $V$ -band magnitude (and is particularly useful since HDF was imaged in  $U$ ,  $B$ ,  $V$  and  $I$  but not  $R$ ).

We obtained the LHS catalog from the SIMBAD data center, and show in figure 1 the reduced proper motion  $H$ , computed in Luyten’s  $R$ -band magnitude  $R_L$  versus his  $m_{\text{pg}} - m_R$  colour index. The disk main sequence (running from upper-left to lower-right) and the disk white dwarf cooling sequence (lower-left) are seen in the figure. There are no sources with  $H > 24$ . Dark halo white dwarfs are expected to have  $H \gtrsim 25$ . We note that there are a few objects in the LHS with  $H > 23.5$ . A literature search using SIMBAD showed that all could be firm identifications as either M dwarfs or disk white dwarfs through parallax, photometry and/or spectroscopic methods (Bessell, 1991, McCook and Sion 1987). We conclude that there are no counterparts in the LHS to the moving sources in the HDF, confirming previous studies (Graff, Laughlin and Freese 1997, Fuchs and Jahreiß 1998, Hansen 1999b).

Richer et al (1999) discuss the colours of the white dwarfs proposed by IRGS99. In the age range of interest, 7 to 15 Gyr, the models have  $V - R$  colours in the range

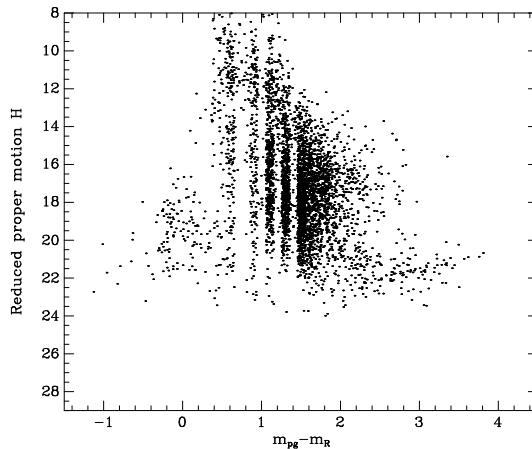


**Figure 1.** The reduced proper motions  $H$  in the Luyten  $R$ -band for the stars in the Luyten Half Second survey versus their colour index ( $m_{\text{pg}} - m_R$ ). No sources are found with  $H > 24$ , where dark halo white dwarfs are expected to lie. Note that the vertical stripes are an artifact due to the limited colour resolution of the LHS survey. A small random number has been added to the Luyten colours to reduce crowding in the figure

$0 < V - R < 0.5$ . We discuss in much more detail the colours of the models in the next section, but at this point if we conservatively adopt  $V - R = 0$ , then the  $V$ -band limit of LHS is (from Eqn 4) is  $V = 18.4$ . Taking this magnitude limit, accounting for the fraction of sky covered,  $\sim 8.5$  sr, and the completeness (60%), the Luyten catalogue probes an effective volume of  $v_{\text{eff}}^{\text{LHS}} = 5700 \text{ pc}^3$  for  $M_V = 17.5$  dark halo white dwarfs. Applying the proper motion window for sources in LHS ( $0.5 < \mu < 2.5$ ) we obtain an survey efficiency of  $\epsilon = 0.22$ , which reduces the effective volume to

$$v_{\text{eff}}^{\text{LHS}} = 1290 \text{ pc}^3 \quad (5)$$

which is much greater than the effective volume of both the KHH survey ( $198 \text{ pc}^3$ ), and the HDF survey ( $95 \text{ pc}^3$ ).

We conclude that the type of objects seen by IRGS99 should be present in significant numbers in the LHS catalog with  $H_R \gtrsim 25$ . The lack of such objects in LHS argues against the interpretation that they are dark halo white dwarfs.

## 4 DISCUSSION

The three surveys are summarised in Table 2. The combined ground-based surveys probe an effective volume which is larger than that probed by HDF by a factor of

$$18 \times 10^{0.6(R_L - I)} \frac{\epsilon_{\text{LHS}}}{\epsilon_{\text{HDF}}} + 1.7 \times 10^{0.6(R - I)} \frac{\epsilon_{\text{KHH}}}{\epsilon_{\text{HDF}}} \quad (6)$$

where  $R_L$  is the Luyten  $R$ -band magnitude,  $\epsilon$  is the survey efficiency, which includes the completeness and the proper motion window, and  $R - I$  is the WD colour.

As can be seen from Eq. 6, the two important parameters in determining the relative strengths of the ground-based surveys to the HDF are the efficiency,  $\epsilon$  and the colour of the dwarfs. We next discuss the effect of the colours of the WDs in detail.

**Table 2.** Summary of the limits of the three experiments discussed in the Paper. The efficiency includes the survey completeness and the probability that an object at absolute magnitude 17.5 will have a proper motion within the proper motion window of the survey

Survey	$\Omega$ str	Mag. limit	Efficiency $\epsilon$
HDF	$3.7 \times 10^{-7}$	$I < 28$	0.42
KHH (i)	$7.6 \times 10^{-3}$	$R < 21.2$	1.00
LHS	8.5	$R_L < 18.5$	0.13

#### 4.1 White Dwarf models

IRGS99 propose that the faint blue sources which they have found in the HDF might be old, hydrogen-atmosphere white dwarfs, which have the surprising property of being blue (Hansen 1999b) due to  $H_2$  opacity (old helium-atmosphere white dwarfs would have cooled so effectively that they would not be visible in any existing survey). Hansen (1999b) has computed  $V$ - and  $I$ -band absolute magnitudes for old white dwarfs for a range of ages. Over the age range of interest, 11 to 16 Gyr, the  $V$ -band absolute magnitude of Hydrogen atmosphere white dwarfs is in the range  $17 \lesssim M_V \lesssim 18$  while the colours lie in the range  $-1 \lesssim V - I \lesssim 1$ . These properties are consistent with the interpretation of the moving HDF objects as old dark halo white dwarfs.

We adopt the models of Hansen (1999b), who kindly made unpublished  $B$  band colours available to us. Other observables of these models are discussed in Richer et al (1999). Within these models, once the temperature of the white dwarf cools below 4000K, the spectral energy distribution becomes extremely non-blackbody. Most of the light is emitted in the  $V$  and  $R$  bands with the peak shifting to the *blue* as the star cools, and the absolute  $M_V$  magnitude of the star stays roughly constant. Thus, the effective volume probed by the photographic catalogues does not strongly depend on models, while the IRGS99 volume, which has an  $I$  band magnitude limit, depends strongly on the temperature of the white dwarf. When computing the relative strengths of the different surveys, the most important parameter is the  $V - I$  colour.

We will discuss three models which cover the  $V - I$  colours of cool white dwarfs. We examined several other models with different ages and white dwarf masses, the three models we discuss illustrate the reasonable parameter space since only the  $V - I$  colour plays a significant role. The three models are denoted O, R and B, where model O, is a fit to the observed candidate white dwarf 4-551, model R represents a dwarf which is red in  $V - I$ , and model B, a dwarf which is blue in  $V - I$ . The parameters chosen for these dwarfs are shown in Table 3.

Note that model R is the reddest possible hydrogen atmosphere dwarf. Both cooler and hotter dwarfs are bluer.

Calculations of effective volumes for different models and different surveys are shown in Table 4. In all cases, the LHS catalogue is the most potent survey, then the KHH survey, and the IGRS survey is the least potent. The combined photographic surveys are 7–18 times as powerful as IRGS99 to  $I = 28$ .

**Table 3.** Three models of halo white dwarfs from Richer et al (1999). We consider a red (“R”) and a blue (“B”) model, and a model which is a match to one of the observed (“O”) objects in the HDF (object 4-551).

Parameter	White Dwarf Model		
	R	O	B
Mass ( $M_\odot$ )	0.66	0.70	0.80
Absolute Magnitude $M_V$	17.49	17.40	18.01
Age (Gyr)	12.0	12.1	12.0
$V - I$	1.10	0.40	0.02
$V - R$	0.96	0.57	0.73

#### 4.2 Combining the surveys

Naïvely, if the object 4-551 detected by IRGS99 is typical of the halo population, there should be tens of dwarfs in the ground-based surveys. Instead, there are none. We calculate the probability of such a mismatch between surveys as follows:

Let  $\lambda$  be the mean expected number of dwarfs seen by IRGS99. We define  $\alpha$  to be the ratio of effective volumes probed by the different surveys:

$$\alpha = \frac{v_{\text{eff}}^{\text{LHS}} + v_{\text{eff}}^{\text{KHH}}}{v_{\text{eff}}^{\text{HDF}}} \quad (7)$$

so that the mean expected number of dwarfs in the combined photographic surveys is  $\alpha\lambda$ . Then the probability that at least one dwarf will be seen in the HDF is  $P_{\text{HDF}} = 1 - e^{-\lambda}$ , while the probability that no dwarfs will be seen in either photographic surveys is  $P_{\text{phot}} = e^{-\alpha\lambda}$ .

The combined probability of both events is

$$P = P_{\text{HDF}} P_{\text{phot}} = (1 - e^{-\lambda}) e^{-\alpha\lambda}. \quad (8)$$

This probability is maximized when

$$\lambda_{\text{max}} = \ln \frac{\alpha + 1}{\alpha} \quad (9)$$

and has a value of

$$P_{\text{max}} = \frac{\alpha^\alpha}{(\alpha + 1)^{\alpha+1}} \sim \frac{1}{e(\alpha + 1)}. \quad (10)$$

Note that, as shown in Table 4, even for the reddest model, where the HDF is relatively most effective, the probability of seeing a star in the HDF and no stars in the more powerful photographic surveys is only 5%. In the case of the actual star observed, 4-551, the probability is lower (2%) that no other stars of the same type would be observed in the photographic surveys.

#### 4.3 Halo Fraction

Having calculated the effective volumes of the surveys, we can calculate the number of dwarfs that would be visible assuming the halo were composed of white dwarfs. This assumption is not entirely consistent with the microlensing results — the MACHO microlensing experiments currently suggest that half the dark halo could be in the form of  $\approx 0.5 M_\odot$  mass objects (Alcock et.al 1997), whereas EROS2 (Afonso et.al, 1999) concludes that objects of this mass can be ruled out at the 95% confidence level. We do not constrain the calculations in this section by these results, but

**Table 4.** The first three rows show the effective volume of the three surveys to the three WD types considered in Table 3. The effective volume includes the survey completeness and the reduction due to the proper motion window. Row 4 shows the combined effective volume of the surveys. Row 5 shows  $N_{\text{WD}}$ , the number of Hydrogen atmosphere white dwarfs expected in the combined surveys (see section 4.3) assuming they make up 50% of the dark halo density. Row 6 shows the ratio of effective volume for the combined ground-based surveys to the HDF survey: they are typically 10-20 times more powerful than the HDF survey. Row 7 shows the (maximised) probability that objects would be detected in the HDF but not detected in the ground-based surveys, and is typically below 5%. The probability has been maximised by fitting for the dark halo mass fraction in white dwarfs, which is shown in row 8.

Description	WD Model		
	R	O	B
$v_{\text{HDF}}^{\text{HDF}} (\text{pc}^3)$	438	189	48
$v_{\text{LHS}}^{\text{eff}} (\text{pc}^3)$	2730	3220	832
$v_{\text{KHH}}^{\text{eff}} (\text{pc}^3)$	403	121	52
Total Volume ( $\text{pc}^3$ )	3571	3530	932
$N_{\text{WD}}$	27	26	7
(LHS + KHH)/HDF	7.2	17.7	18.4
Probability	5.0%	2.0%	2.0%
Halo Fraction	2.0%	2.0%	3.0%

rather use the results of the HDF proper motion search itself as our starting point. We adopt a local halo density of  $0.0076 M_{\odot} \text{pc}^{-3}$  and assume that 50% of this density is due to Hydrogen atmosphere white dwarfs. We assume that the remaining 50% of the dark halo is in helium atmosphere white dwarfs, which will have cooled far below the detection limits of the surveys.

The number of hydrogen atmosphere white dwarfs expected in the combined surveys  $N_{\text{WD}}$  is shown in row 5 of Table 4. The probability that one or more white dwarfs would be seen in HDF while none are seen in the photographic surveys is very low for all the models. Using equation 8, all three models in which Hydrogen atmosphere white dwarfs make up half of the dark halo can be ruled out with greater than 99% confidence.

We tested models in which the dark halo white dwarf fraction maximises the probability that one or more white dwarfs would be seen in HDF while none are seen in the photographic surveys (Eqns 9 and 10). Model R has the highest probability of explaining the combined survey results, albeit with a low probability of only 5% and a dark halo white dwarf fraction of just 2.0%. For the other two models the probability of there being at least one object in HDF and none in the ground based surveys is  $P_{\text{max}} = 2\%$ , and the corresponding fraction of dark halo white dwarfs is also very low, less than 3%.

#### 4.4 Survey in progress: EROS-II Wide Field Imager

A  $V$ -band limit on the luminosity of putative dark halo white dwarfs has been set by Goldman (1999), using the first 140 square degrees of the EROS-II survey (a  $V$  and  $I$  band wide field imager), which will cover 350 square de-

grees and reach  $I \approx 20.5$  and  $V \approx 21.5$  when completed. No high proper motion objects were detected, and Goldman (1999) uses this to set a  $V$ -band absolute magnitude limit of  $M_V > 17.2$  on dark halo WDs. This is consistent with the Ibata et al proposed WDs, since they lie in  $17 \lesssim M_V \lesssim 18$ . The survey is currently approaching completion and will be very sensitive to nearby white dwarfs, surveying some 5000  $\text{pc}^3$  (Goldman, private communication).

## 5 CONCLUSIONS

Ibata et al (1999) have recently discovered faint moving objects in the Hubble Deep Field, proposing that these might be cool white dwarfs making up the entire mass of the Galactic dark halo. We have searched for nearby counterparts to these objects in a number of ground-based proper motion surveys. No such objects have been found, even though the combined photographic surveys are tens of times more powerful than the HDF. The probability of this occurring is quite low,  $< 5\%$ , even in the most conservative model. This study leads us to the conclusion that it is unlikely that hydrogen atmosphere white dwarfs make up a significant fraction of the halo dark matter. No limits can be placed yet on helium atmosphere dwarfs from optical searches.

## ACKNOWLEDGMENTS

We thank Bertrand Goldman, Andy Gould, Geza Gyuk, Nigel Hambly, Hartmut Jahrei, Harvey Richer and Ali Talib for help and interesting discussions. Brad Hansen shared his unpublished calculations of  $B$ -band colours of cool white dwarf atmospheres. This research was supported in part by the Academy of Finland, and by Danmarks Grundforskningsfond through its support for the establishment of the Theoretical Astrophysics Center. We have made extensive use of the SIMBAD astronomical data base for which we are very grateful.

## REFERENCES

- Afonso, et.al. (The EROS Collaboration), 1999, A&A, 344, L66
- Alcock C. et al. 1997, ApJ, 486, 697
- Bessell, M. S. 1991, AJ, 101, 662
- Chabrier, G. 1999, ApJ, 513, 103
- Conti, A., Kennefick, J. D., Martini, P. & Osmer, P.S. 1999, AJ, 117, 645
- Dawson, P. C. 1986, ApJ, 311, 984
- Evans, D. W., 1992, MNRAS, 255, 521
- Fields, B., Freese, K. & Graff, D.S., 1998, New Astro., 3, 347
- Fields, B., Freese, K. & Graff, D.S., 1999, ApJ, in press
- Fuchs, B. and Jahrei H. 1998, A&A 329, 81
- Gliese, W. and Jahrei H. 1980, A&A 85, 350
- Goldman, B. 1999, 3rd Stromlo Symposium, The Galactic Halo, ASP Conference Series, Vol 165, p413, B. Gibson, T. Axelrod, M. Putman Eds.
- Graff, D.S., Laughlin, G., & Freese, K., 1998, ApJ, 499, 7
- Graff, D.S., Walker, T.P., Freese, K. & Pinnsonneault, M.H., 1999, ApJ, 523, 77
- Hambly, N. C., Smartt, S. J., Hodgkin, S. T., Jameson, R. F., Kemp, S. N., Rolleston, W. R. J. & Steele, I. A. 1999, MNRAS, 309, L33
- Hansen, B. 1999a, ApJ, 517, 39

- Hansen, B. 1999b, *ApJ*, 520, 680  
Harris, H. C., Dahn, C. C., Vrba, F. J., Henden, A. A., Liebert, J., Schmidt, G. D. & Reid, I. N. 1999, *ApJ*, 524, 1000  
Hodgkin, S.T., Oppenheimer, B.R., Hambly, N.C., Jameson, R.F., Smartt, S.J., Steele, I.A. 1999, preprint  
Ibata, R., Richer, H., Gilliland, R. & Scott, D. 1999, *astro-ph/9908270* (IRGS99)  
Knox, R., Hawkins, M. & Hambley, N. 1999, *MNRAS*, 306, 736 (KHH)  
Luyten, W. & La Bonte, A., 1973, *The South Galactic Pole*, Univ. of Minnesota, Minneapolis  
Luyten, W., 1922, *Lick Obs Bull*, No. 336  
Monet, D. 1998, *BAAS*, 193, 120.03  
McCook, G. P. & Sion, E. M. 1987, *ApJS*, 65, 603  
Richer, H.B., 1999, *astro-ph/9906424*  
Richer, H.B., Hansen, B., Limongi, M., Chieffi, A., Straniero, O. & Fahlman, G. G. 1999, *ApJ*, in press, *astro-ph/9908337*  
Salim, S. & Gould, A. 1999, *astro-ph/9909455*

## APPENDIX A: COMPLETENESS OF NLTT

In this section we perform a statistical test to investigate the completeness of the faint end of NLTT down to its nominal cutoff of  $\mu_1 = 200 \text{ mas yr}^{-1}$ . In the test we assume that the local luminosity function is constant, and that the number density of stars does not change appreciably on scales equivalent to a distance modulus of 0.5 mag.

Consider two spheres centered around the Sun, the volumes of which stand in ratio 2:1. This is equivalent to radii being in relation  $r_1/r_2 = 1.259$ , or distance modulus difference of 0.5 mag. If we define the outer edge of the bigger sphere as the distance at which a star of apparent magnitude  $R_{L,1}$  produce a proper motion  $\mu_1 = 200 \text{ mas yr}^{-1}$ , then this same star, if placed at distance  $r_2$ , would have a proper motion of  $\mu_2 = \frac{r_1}{r_2} \mu_1 = 252 \text{ mas yr}^{-1}$ . Also, it would be 0.5 mag brighter. Therefore,  $\mu_2$  defines a proper motion limit at the distance  $r_2$  that is equivalent to proper motion limit  $\mu_1$  at  $r_1$ . These are the lower limits. However, in NLTT there is also an upper proper-motion cutoff of  $\mu_2^{\text{lim}} = 2500 \text{ mas yr}^{-1}$ . If we adopt this as a limit, this corresponds to some inner boundary of the smaller sphere (which we can now call a shell). Everything closer than this inner boundary would have  $\mu > \mu_2^{\text{lim}}$  and would not be included in NLTT. Now, in order to keep volumes of both shells in appropriate ratio, the outer sphere (shell) has to have an inner edge corresponding to a proper motion of  $\mu_1^{\text{lim}} = \frac{r_2}{r_1} \mu_2^{\text{lim}} = 1986 \text{ mas yr}^{-1}$ .

Now that we have defined the two shells in terms of the limiting proper motions, the statistical test consists of comparing the number of stars  $N_1$  of a given magnitude  $R_L$  (in a  $\Delta R_L = 0.5$  mag bin) in the outer shell ( $200 \text{ mas yr}^{-1} < \mu < 1986 \text{ mas yr}^{-1}$ ), with the number of stars  $N_2$  of a magnitude  $R_L - (R_{L,1} - R_{L,2}) = R_L - \Delta R_L = R_L - 0.5$  in the inner shell ( $252 \text{ mas yr}^{-1} < \mu < 2500 \text{ mas yr}^{-1}$ ). The 0.5 mag shift (equal to one bin) brings the absolute magnitudes of stars in the outer shell to that of the inner shell. The measure of completeness at magnitude  $R_L$  is given by the ratio

$$f(R_L) = \frac{N_1(R_L)}{N_2(R_L - 0.5)}. \quad (\text{A1})$$

If the sample of stars of apparent magnitude  $R_L$  is 100% complete with respect to those of  $R_L - 0.5$ , then  $f(R_L) \equiv (r_1/r_2)^3 = 2$ . Now we can define the complete-

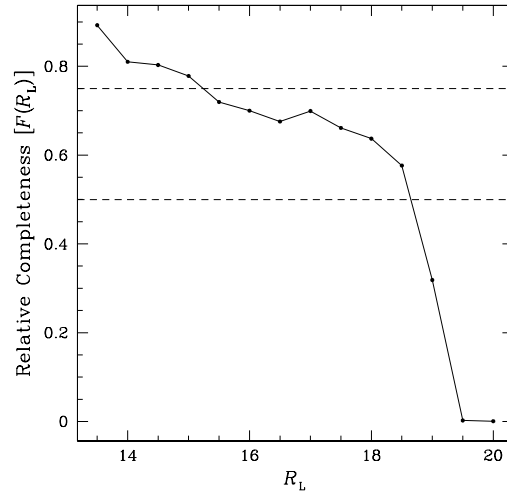


**Figure A1.** Completeness of NLTT relative to  $R_L = 13$ , in the Completed Palomar Region ( $\delta \gtrsim -33^\circ$ ,  $|b| > 10^\circ$ ). Dashed lines show 75% and 50% completeness levels.

ness function  $F(R_L)$  for the stars of apparent magnitude  $R_L$ , in the following way

$$F(R_L) = \prod_{R'_L=R_L}^{R'_L=R_L+\Delta R_L} \frac{f(R'_L)}{2}, \quad (\text{A2})$$

where  $R_{L,\text{comp}}$  is some bright apparent magnitude at which we believe the catalogue is complete.

In Figure A1 we show the completeness function  $F(R_L)$  for the faint end of NLTT. More specifically, the test was performed on the subsample of NLTT that is believed to be spatially complete, that is, the part called the Completed Palomar Region (CPR) by Dawson (1986). This region covers northern declinations ( $\delta \gtrsim -33^\circ$ ), and avoids the galactic plane ( $|b| > 10^\circ$ ). We take  $R_{L,\text{comp}} = 13$ . The choice is somewhat arbitrary, but we have reasons to believe that NLTT is complete at this magnitude. First, when we plot  $f(R_L)$  against  $R_L$ , we get a flat region around  $R_L = 13$ . Going to still brighter magnitudes might bring us into the part of NLTT that was not compiled from the photographic plates. Therefore, Figure A1 shows the completeness of  $R_L$  with respect to  $R_L = 13$ . Dashed lines represent 75% and 50% completeness levels. The completeness drops gradually from 90% at  $R_L = 13.5$  to 60% at  $R_L = 18.5$ .

## APPENDIX B: PHOTOMETRIC CALIBRATION OF NLTT

Throughout the previous section we used Luyten's red magnitude  $R_L$ . We derive here a calibration of  $R_L$  to standard Johnson magnitudes.

NLTT magnitudes are given as photographic (blue plate) and red plate magnitudes. The Hipparcos catalog contains most of the NLTT stars to its detection limit ( $V \sim 12$ ). We matched NLTT stars with the corresponding Hipparcos stars (details are given in Salim & Gould 1999), and found 6084 matches with the complete photometric infor-

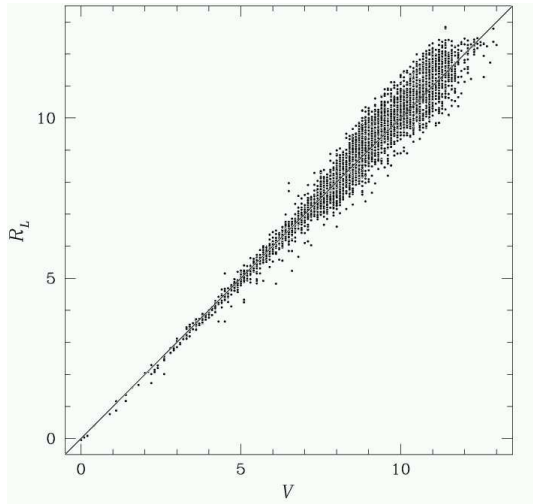


**Figure B1.** Luyten’s “red” magnitude  $R_L$  versus Johnson  $V$  magnitude for stars in both NLTT and Hipparcos catalogs. A 1:1 line is shown for reference.

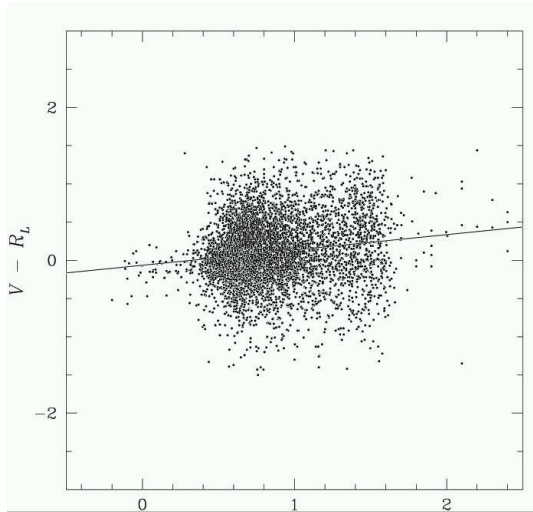


**Figure B2.** Residuals between Luyten’s  $R_L$  magnitude and Johnson  $V$  magnitude plotted against the Johnson  $B - V$  colors of the stars that appear in both NLTT and Hipparcos catalogs. The best-fit line is the calibration given in Equation B1.

mation. These stars therefore calibrate the bright end of NLTT ( $0 < V < 12.5$ ), as follows:

$$V = R_L - 0.06 + 0.200(B - V) \quad (\text{B1})$$

and

$$V = R_L - 0.08 + 0.196(B_L - R_L), \quad (\text{B2})$$

where  $B_L$  and  $R_L$  are NLTT’s blue (photographic) and red magnitudes, respectively. The first relation is shown graphically in Figure B2. From the first relation we can see that both Johnson  $V$  and Luyten’s  $R_L$  have almost the same zero points. More importantly, the low color term of 0.2 puts  $R_L$  magnitudes much closer to  $V$  than to standard Kron  $R$ . This is in sharp contrast to Dawson (1986) who finds that  $R_L$  and Kron  $R$  are almost the same, with the only difference being in zero point. Dawson’s calibration would give a

colour term coefficient of about 0.6 in eq. B1, not 0.2 that we obtain. RMS in both equations B1 and B2 are 0.40 mag. We cannot account for this discrepancy, but note that it would not change the main conclusions of the paper.

The calibration above is restricted to the bright end of NLTT. Obtaining a calibration for the fainter part was somewhat more complicated. Our faint end calibration is based on the USNO-A2.0 all-sky astrometric survey (Monet 1998). Although USNO-A2.0 itself does not contain standard magnitudes, it can be calibrated independently (see Salim & Gould 1999). The USNO-A2.0 catalog’s photometric accuracy ( $\approx 0.25$  mag) is far superior to NLTT’s photometry ( $\gtrsim 0.5$  mag). The complicated step is finding faint NLTT stars in the USNO-A2.0 catalog. This procedure is also described in Salim & Gould (1999). In the end, we identify 33286 NLTT stars (in the northern,  $\delta > -15^\circ$ ) part of the sky) in USNO-A2.0. Out of this number, 21053 stars have  $V > 15$  and we use them to construct the calibration. We obtain the following relation

$$V = R_L + 0.01 + 0.230(B - V) \quad (\text{B3})$$

with an RMS scatter of 0.47 mag. This confirms the calibration obtained at the bright end, and reaffirms our suggestion that  $R_L$  is closer to  $V$  than to Kron  $R$ . We use calibration from eq. B1 throughout this paper.